Hindawi
Advances in Materials Science and Engineering
Volume 2022, Article ID 5687407, 8 pages
https://doi.org/10.1155/2022/5687407

Research Article

Residual Stress Distribution in Selective Laser Melting of SS316L Parts

Harinadh Vemanaboina,[1] **Paolo Ferro**,[2] **B. Sridhar Babu**,[1] **Edison Gundabattini**,[3] **Kaushik Kumar**,[4] **and Filippo Berto**[5]

[1]*Department of Mechanical Engineering, Sri Venkateswara College of Engineering & Technology (Autonomous), Chittoor 517127, Andhra Pradesh, India*
[2]*Department of Engineering and Management, University of Padua, Stradella San Nicola, Vicenza 36100, Italy*
[3]*Department of Thermal and Energy Engineering, School of Mechanical Engineering, Vellore Institute of Technology, Vellore 632014, India*
[4]*Department of Mechanical Engineering, Birla Institute of Technology, Mesra, Ranchi, India*
[5]*Department of Engineering Design and Materials, Norwegian University of Science and Technology, Trondheim 7491, Norway*

Correspondence should be addressed to B. Sridhar Babu; bsridhar7777@cmritonline.ac.in

Received 2 June 2022; Revised 1 July 2022; Accepted 5 July 2022; Published 31 July 2022

Academic Editor: Alicia E. Ares

Additive manufacturing is one of the fastest-growing fields in materials engineering. This is because there is a new trend for custom, high-precision, and on-demand manufacturing. The undesired residual stress induced in the components during layer-by-layer melting and solidification of the metal powder is an important issue related to the selective laser melting (SLM) process that needs to be studied deeply. These stresses may impair mechanical performance and potentially result in premature failure. As a result, a thorough knowledge of residual stress is crucial for improved component dependability. By keeping constant process parameters, samples were produced with a difference in the scanning method. Results indicate that the defect-free parts are manufactured in all the four patterns used, and the self-balanced residual stresses are within the safe limits of yield strength.

1. Introduction

Additive manufacturing techniques, such as selective laser melting (SLM), are used to create complex components that may be customised in a variety of ways, such as topological optimization, lightweight construction, and lattice architectures. The mechanical characteristics of SLM components are almost identical or even better than those of bulk material provided the components are near full density [1]. It is possible to construct functional metal goods using selective laser melting (SLM) in which a computer model serves as a guide for melting metal particles layer by layer [2]. SLM has a broad variety of applications in aerospace, automotive, tool, medical, and power generation sectors because of its promise of quick production. LPBF enables successive layer assembly with a laser beam as the heat source. The localized heat input in micron length and time scale induces rapid melting and consolidation through the formation of a molten metal pool [3]. Unfortunately, the enhanced thermal cycle of quick melting, cooling, and melt-back during SLM leads to higher residual stress gradients, which contribute to molten pool configuration, microstructure and mechanical properties microcracks, delamination, and component deformation, all of which are major challenges in the metal additive manufacturing (AM) community [4]. It is recalled that residual stress (RS) originates from differential expansion and contraction of the material [5, 6].

Residual stress then causes deformation, delamination, and fissures in the component. Additional faults might emerge throughout the SLM process. Apart from RS, the most prevalent faults are balling, warping, and dross development [7–11]. However, RS may have similar effects to

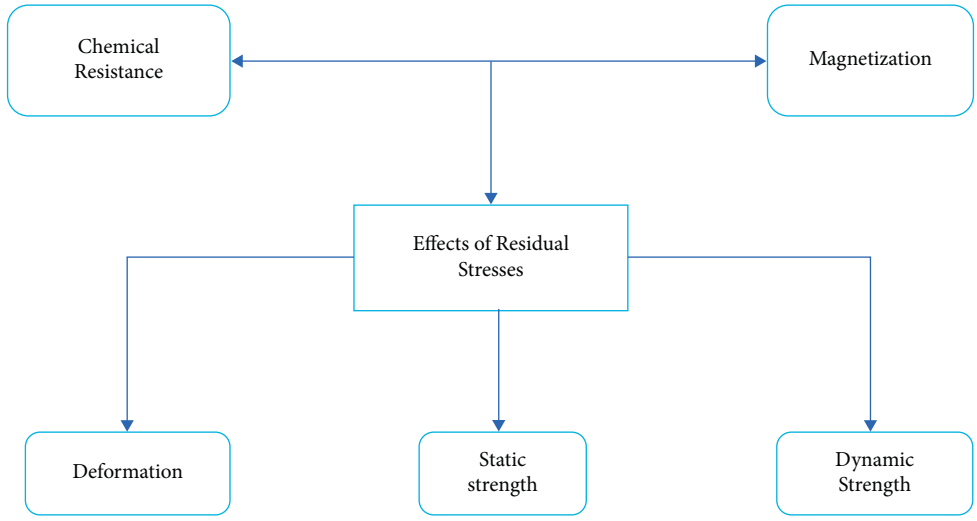

Figure 1: Residual stress effects in materials (adapted from ref. [17]).

stress concentration that are vital to component life cycle. The presence of RS, along with additional loading stress, may dramatically weaken fatigue resistance and induce deformation, as well as delamination, fissures, and other structural problems [12–15]. Residual stresses are self-balancing stresses that remain in a component after manufacture, even in the absence of a temperature gradient or external forces. These stresses are created by geometric mismatches between components covering many locations and phases inside a part, or even by local variances in elastic constants, thermal, and mechanical properties [16].

In addition to decreased fatigue resistance and critical failure, while in operation, RS has other negative effects, as illustrated in Figure 1. Chemical resistance, magnetization, deformation resistance, and static and dynamic strength are just a few of the properties that are affected [17]. Sintering/melting and subsequent solidification of metal may be induced by laser, electron, or plasma heating. There is a change in how each component functions locally as a result [18]. It is possible that rapid cooling and heating may cause distortions and cracks in AM materials. RS is also responsible for additively manufactured components' anisotropic behavior [19]. In Figure 2, the temperature gradient mechanism (TGM) may be observed as a predecessor to residual stresses in AM. This means that, during localized heating, the power source increases stress in the region around it as well as a sequence of local deformations (expressed by its deformation values). During subsequent cooling of the molten top layer, thermal contraction induces tensile residual stresses on the solidified zone and compressive residual stresses at its boundary due to the self-balancing character of the RS field [15, 20]. Because of the intricacy of the AM process, the TGM model can only provide a simplified representation of where and how residual stresses are generated [21]. RS intensity and material parameters such as grain size, heat capacity, porosity, and phase composition, as well as process variables such as laser/electron beam power, preheating type, scan techniques and speed, and layer thickness, are all linked [16, 18, 22].

The influence of the print scan method on residual stresses is studied utilizing an SLM procedure. The bridge-shaped samples made of AISI316 L stainless steel were created and then tested. The current work is focused on analyzing as-printed SLM specimens in order to get sufficient primary knowledge regarding the surface and interior quality of the samples. XRD is used to quantify residual stresses. These findings would contribute to a better understanding of the evolution of residual stress during SLM using four different pattern techniques.

2. Materials and Methods

A TruPrint 1000 SLM equipment was utilised to create the stainless steel 316L samples used in this investigation. The laser has a concentrated beam diameter of 20 μm. Both samples were created in a 99.999% pure argon atmosphere to prevent oxidation during the SLM process. The basic material powders had a spherical form and varied in size from 20 to 40 μm. Table 1 collects the values of process parameters employed in this study such as laser power (W), scan speed (mm/s), and layer thickness (μm). Samples were produced with four different scanning strategies as shown in Figure 3. For each one, four samples were made at a time utilizing the built area, and all were subjected to the required test. The result provides the mean value obtained with very negligible standard deviation. This ensured the reliability and repeatability of the output. Software associated with the additive manufacturing machine used has an option of dry run which suggests the best orientation on the basis of material used, run time, etc. So, while placing the model for building, orientation considered is given with dimensions and geometry same as depicted in Figure 4(a). In this case, support material was used in the first few layers and below the hump in the product [23, 24]. Their bridge-like shape is specially designed to evaluate residual stresses of metal parts built via SLM.

The photos in Figure 4(b) show examples of SS316 L printed samples as a function of scan strategy used to

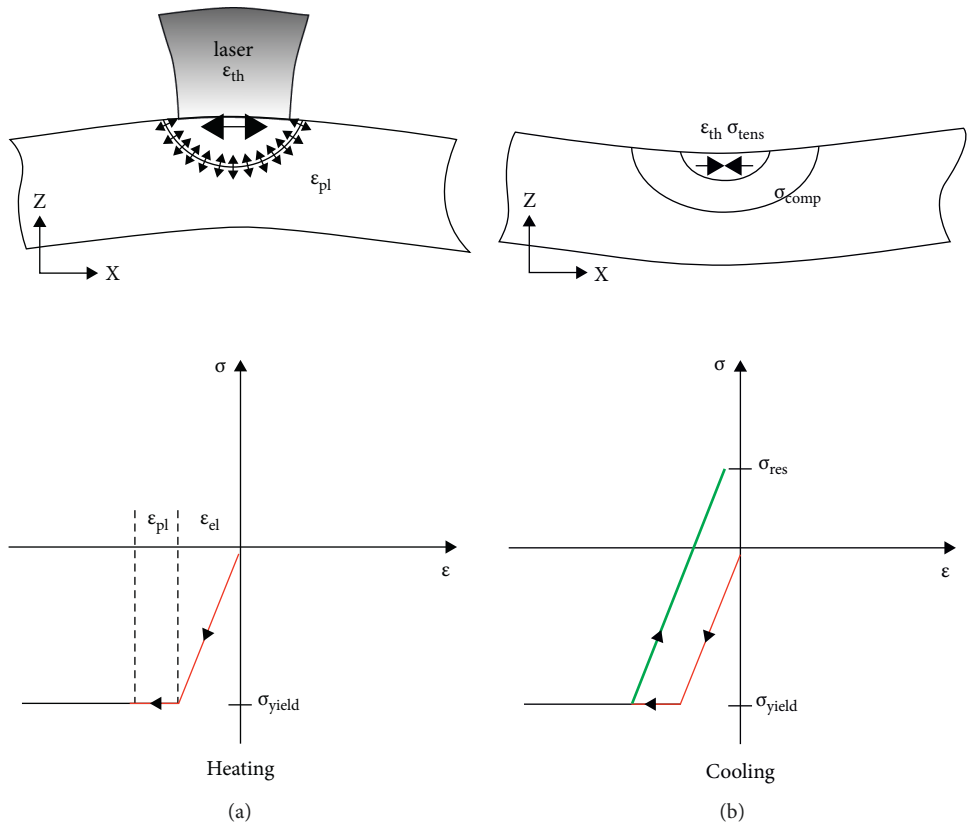

Figure 2: Mechanism of temperature gradient (TGM). Stresses and deformation during heating (a) and cooling down (b) in the irradiated zone [20].

Table 1: SLM process parameters used to build samples.

S. no.	Build parameter (units)	Value
1	Laser power (W)	130 W
2	Laser beam diameter	55 μm
3	Scanning speed	500 mm/sec
4	Powder grain size	20 to 40 μm
5	Layer thickness	40 μm
6	Process time per specimen	3 h
7	Hatch distance	80 μm

produce them. According to the ASME SEC-VIII standard, the additively manufactured specimens were analyzed to search for macrodefects using the X-ray radiography technique. Potential radiographic black patches are caused by internal defects such as porosity, blowholes, or fractures. These flaws were not detected in the analyzed samples as shown in Figure 5. Vickers hardness was performed on the components using the ASTM E-384-16 standard. The cold mounted specimens were used for testing. 1 kg load was employed with an indentation dwell time of 8 sec.

In this study, RS is measured on the lateral surface at different positions using the Pulstec μ-X360n portable X-ray residual stress analyzer. Figure 6 shows both the instrument and the camera image in the three different positions of the specimen. The sample surface was cleaned using emery sheets before measurement. cos(α) measuring method with a spot size of 2 mm was adopted. Sample measuring parameters are the diffraction angle (156.396°), interplanar spacing (d = 1.170 Å), X-ray wavelength (Cr), K-alpha (2.29093 Å), and K-beta (2.08480 Å).

3. Results and Discussion

3.1. Hardness. Vickers hardness measurements were performed on the top and transverse surfaces of as-fabricated samples shown in Figure 4. The hardness results depend on the four different scanning strategies used to print the parts. The chess field pattern gives the highest hardness average value of 303 HV, and the lowest for anti-parallel horizontal is 227 HV [13, 14]. The hardness values were obtained. The increase in the hardness was attributed to the repeated thermal cycles experienced during the multilayered procedure with melting and solidification. SLM samples had higher average hardness values than those of the cast samples (227, 303, 259, and 271 HV) (192 HV). Different studies [10, 15–17] have confirmed that additively manufactured SS316 L components have a greater hardness than that of SS316 L components traditionally fabricated.

3.2. Residual Stresses. The residual stress field of metal AM components is affected by scanning techniques, dwell duration, and a variety of other process factors that have a significant influence on thermal history. Wu et al. [25] had measured the residual stress in AISI316 stainless steel produced by SLM by using an imaging method called digital

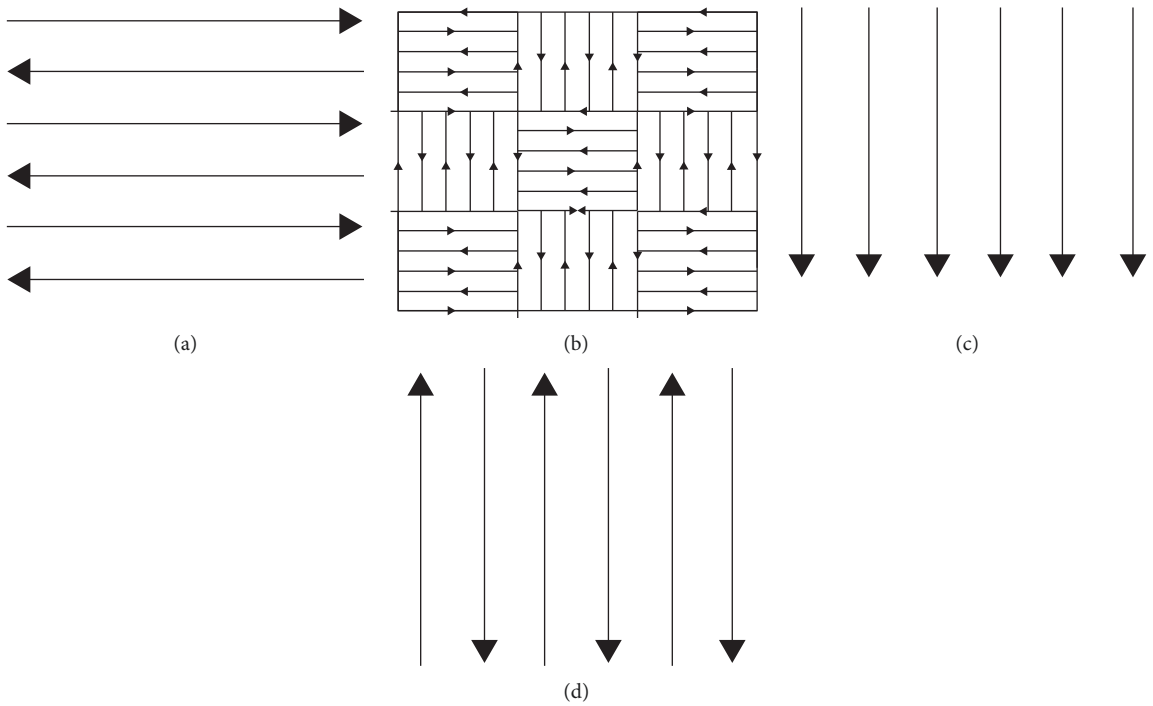

Figure 3: Scanning strategies: (a) antiparallel horizontal, (b) chess field, (c) unidirectional, and (d) bidirectional.

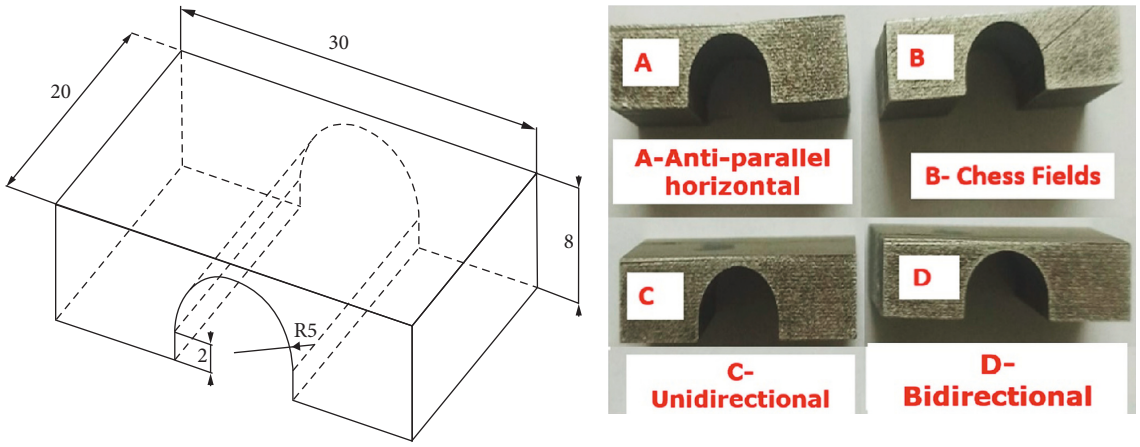

Figure 4: (a) Dimensions of the bridge construction and (b) final product from SLM.

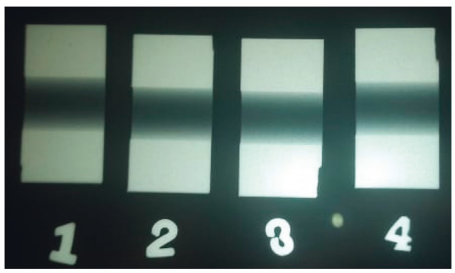

Figure 5: X-ray radiography of the printed components.

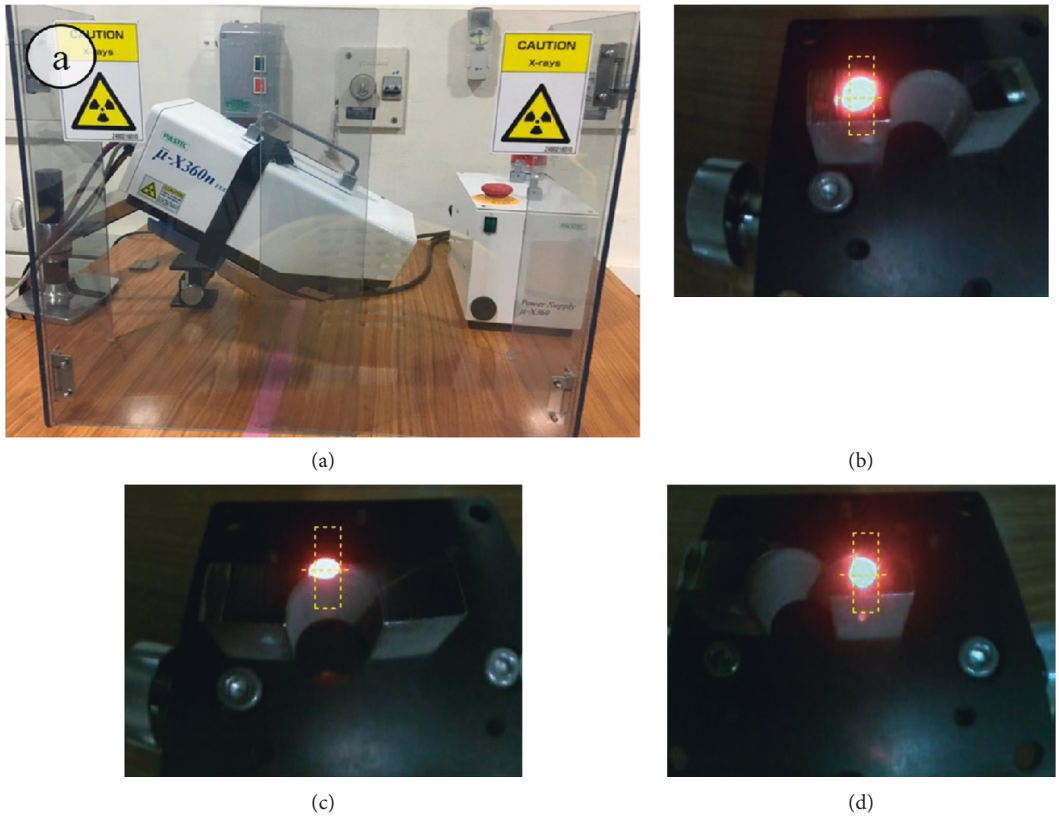

Figure 6: Residual stress analyzer (a) and camera image of measuring surface (b, c, and d).

image correlation (DIC) and XRD. There has been a great deal of research into the dependency of residual stress on aspects such as scanning method, laser power, scanning speed, and construction orientation. A smaller scan island and a higher energy density throughout the length of the scan island would result in a reduced residual stress field. Tensile residual stress in the build direction of a cut-off component in the as-built condition is found immediately under the top surface, followed by a compressive zone in the center and a tensile zone at the bottom surface, according to Mercelis and Kruth [16].

At the build substrate interface, residual stress in SLM manufactured stainless steel and Ti6Al4V small samples was found to be more tensile than that in the perpendicular direction, according to Yadroitsev and Yadroitsava [26]. For the SLM-produced item, Kruth et al. [20] used the bridge curvature technique to measure residual stress. Residual stress of SLM-processed components may be quickly analyzed using this method [27, 28]. The angle of curvature of the bridge's two bottom surfaces after it has been removed from the substrate determines the amount of residual stress in the bridge-shaped portion. For decreasing residual stress and deformation during the SLM process, shorter scan vectors and a larger rotation angle were recommended.

As fabricated samples have undergone the residual stresses measured on the surface as shown in Figures 6(b)–6(d)), antiparallel horizontal pattern induces compressive residual stresses at the middle and tensile in nature at other two ends, with a variation from −5 MPa to 14 MPa, as shown in Figure 7(a). In the chess field pattern, the stresses were tensile in nature throughout the measured surface as given in Figure 7(b); they vary from a minimum of 20 MPa at the left side end to a maximum of 101 MPa at the middle of the fabricated part. In Figure 7(c) (unidirectional scanning strategy), compressive residual stresses were measured on either side of the parts; their values are −20 MPa at the left side and −34 MPa at the right side with maximum of 43 MPa in between.

Compared to other scanning strategies, the bidirectional pattern has induced a nonsymmetric residual stress pattern (Figure 7(d)) with a residual stresses value of −25 MPa at the right side and 9 MPa at the left side of the part. Due to the complex thermal history the workpiece undergoes during the additive manufacturing process, it is extremely difficult to predict the residual stress induced in a particular position of the workpiece that was subjected to repeated heating and cooling of different intensities depending on the scanning strategy applied. This work demonstrated that residual stress is highly dependent on the raster strategy, and for the geometry and process parameters used, its values are well below the yield stress of the material under investigation (170 MPa). Despite different works present in the literature covering this topic [16, 20, 25–27], experimental measurements of residual stress in additively manufactured component are still scarce. This work aims at covering this gap and putting some basis for a better comprehension of this emerging technology.

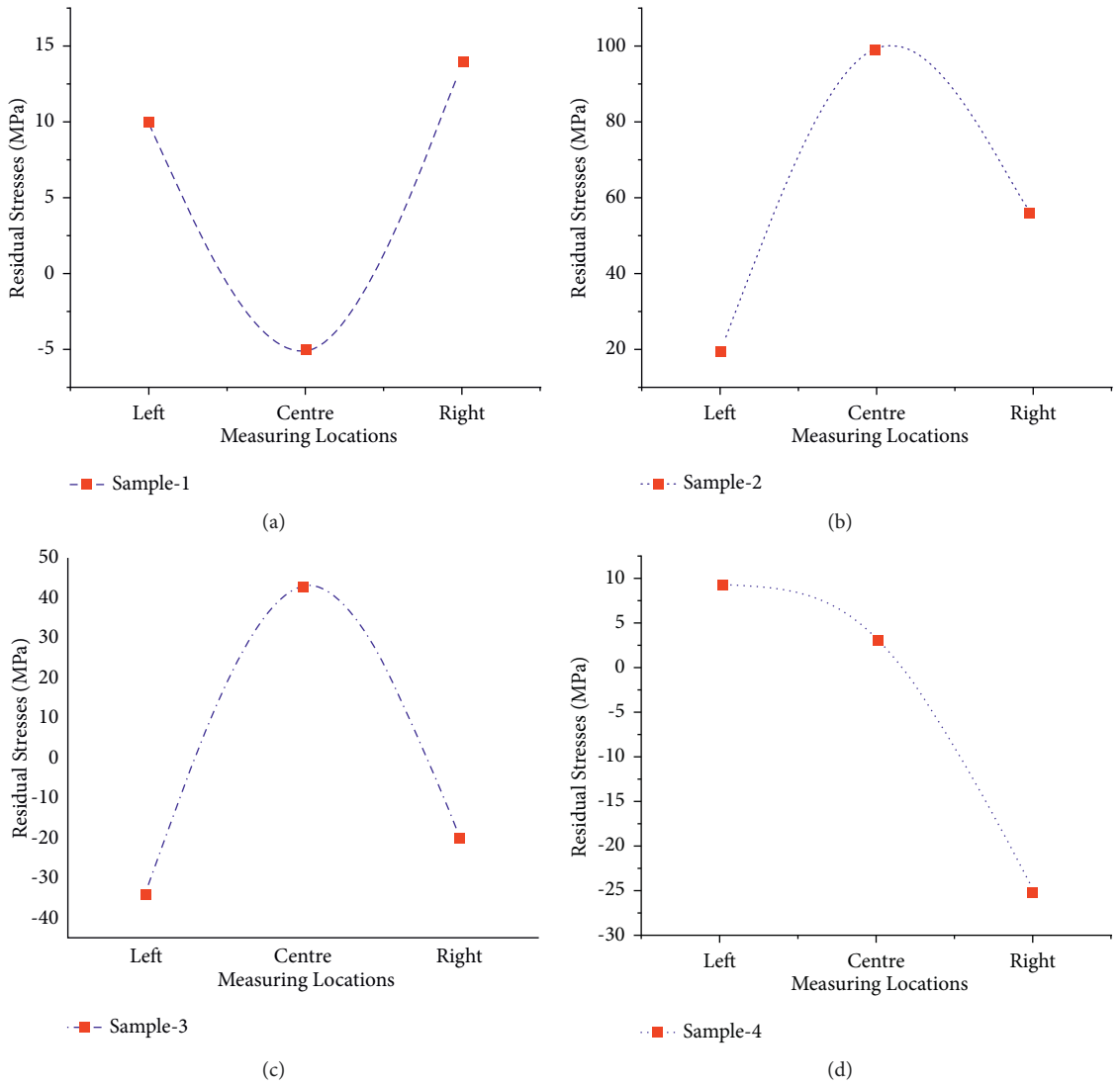

Figure 7: Residual stress distribution as a function of scanning strategy: (a) antiparallel horizontal, (b) chess field, (c) unidirectional, and (d) bidirectional.

4. Conclusions

In this study, the formation of residual stress as a function of pattern strategies in metal additive manufacturing was analyzed. The important outcomes of this effort are summarized as follows:

(i) Defect-free 3D metal printed parts were produced irrespective to the scanning strategy used.

(ii) SLM parts show higher hardness values than those of the cast parts.

(iii) Residual stresses in all the printed parts are found within the yield limits of the base materials with a good factor of safety.

(iv) Metal AM residual stress may be reduced via preheating, process planning, feedback management, and laser peening. Residual stress relief is best achieved by machining and heat treatment.

The research on residual stress in AM is still in its early stages. In the future, researchers will look into how to incorporate the rotation of the scanning strategy between the layers [29, 30] to measure macro- and microresidual stresses, as well as the effects of crystal structure, simulation, postprocess mitigation, fatigue, creep, and corrosion on the size and function of 3D-printed parts.

Data Availability

All the data or models analyzed during the study are included in this published article.

Conflicts of Interest

The authors declare that there are no conflicts of interest regarding the publication of this paper.

Acknowledgments

The authors are thankful to the management of the Vellore Institute of Technology (VIT), Vellore, for enabling us to conduct residual stress measurements using Pulstec residual stress analyzer test in the advanced material processing and testing lab. The authors also thank Akella Systems, Hyderabad, for their support.

References

[1] R. M. Baitimerov, P. A. Lykov, L. V. Lykov, and E. V. Radionova, "Parameter optimization for selective laser melting of TiAl6V4 alloy by CO2 laser," *Bulletin of the South Ural State University series "Mechanical Engineering Industry"*, vol. 17, no. 03, pp. 36–40, 2017.

[2] J. Kruth, M. Leu, and T. Nakagawa, "Progress in additive manufacturing and rapid prototyping," *CIRP Annals*, vol. 47, no. 2, pp. 525–540, 1998.

[3] W. Yu, Z. Xiao, X. Zhang et al., "Processing and characterization of crack-free 7075 aluminum alloys with elemental Zr modification by laser powder bed fusion," *Materials Science in Additive Manufacturing*, vol. 1, no. 1, p. 4, 2022.

[4] H. Zhang, D. Gu, and D. Dai, "Laser printing path and its influence on molten pool configuration, microstructure and mechanical properties of laser powder bed fusion processed rare earth element modified Al-Mg alloy," *Virtual and Physical Prototyping*, vol. 17, no. 2, pp. 308–328, 2022.

[5] R. J. WilliamsWilliams, C. M. DaviesDavies, P. A. HooperHooper, and P. A. Hooper, "A pragmatic part scale model for residual stress and distortion prediction in powder bed fusion," *Additive Manufacturing*, vol. 22, pp. 416–425, 2018.

[6] C. Li, J. F. Liu, and Y. B. Guo, "Prediction of residual stress and Part Distortion in selective laser melting," *Procedia CIRP*, vol. 45, pp. 171–174, 2016.

[7] C. Hardes, F. Pöhl, A. Röttger, M. Thiele, W. Theisen, and C. Esen, "Cavitation erosion resistance of 316L austenitic steel processed by selective laser melting (SLM)," *Additive Manufacturing*, vol. 29, Article ID 100786, 2019.

[8] O. B. Kovalev and A. M. Gurin, "Multivortex convection of metal in molten pool with dispersed impurity induced by laser radiation," *International Journal of Heat and Mass Transfer*, vol. 68, pp. 269–277, 2014.

[9] Y. Qiu, J. Wu, A. Chen et al., "Balling phenomenon and cracks in alumina ceramics prepared by direct selective laser melting assisted with pressure treatment," *Ceramics International*, 2020.

[10] J. T. Black and R. A. Kohser, *Materials and Process Inmanufacturing*, John Wiley & Sons, New Jersey, NJ, USA, 2012.

[11] G. R. Kumar, M. Sathishkumar, M. Vignesh et al., "Metal additive manufacturing of commercial aerospace components - a comprehensive review," *Proceedings of the Institution of Mechanical Engineers - Part E: Journal of Process Mechanical Engineering*, Article ID 095440892211040, 2022.

[12] W. E. Frazier, "Metal additive manufacturing: a review," *Journal of Materials Engineering and Performance*, vol. 23, no. 6, pp. 1917–1928, 2014.

[13] V. Trufyakov, P. Mikheev, and Y. Kudryavtsev, "Fatigue strength of welded structures," in *Residual Stresses and Improvement Treatments*Harwood Academic Publishers, Reading, UK, 1995.

[14] Y. Kudryavtsev, *Effect of Residual Stresses on the Endurance of Welded Joints*, pp. 1568–1594, International Institute of Welding, Paris, 1994.

[15] D. D. Gu, W. Meiners, K. Wissenbach, and R. Poprawe, "Laser additive manufacturing of metallic components: materials, processes and mechanisms," *International Materials Reviews*, vol. 57, no. 3, pp. 133–164, 2012.

[16] P. Mercelis and J. P. Kruth, "Residual stresses in selective laser sintering and selective laser melting," *Rapid Prototyping Journal*, vol. 12, no. 5, pp. 254–265, 2006.

[17] E. Brinksmeier, J. T. Cammett, W. König, P. Leskovar, J. Peters, and H. K. Tönshoff, "Residual stresses - measurement and causes in machining processes," *CIRP Annals*, vol. 31, no. 2, pp. 491–510, 1982.

[18] J. P. Kruth, L. Froyen, J. Van Vaerenbergh, P. Mercelis, M. Rombouts, and B. Lauwers, "Selective laser melting of iron-based powder," *Journal of Materials Processing Technology*, vol. 149, no. 1-3, pp. 616–622, 2004.

[19] N. S. Rossini, M. Dassisti, K. Y. Benyounis, and A. G. Olabi, "Methods of measuring residual stresses in components," *Materials & Design*, vol. 35, pp. 572–588, 2012.

[20] J. P. Kruth, J. Deckers, E. Yasa, and R. Wauthlé, "Assessing and comparing influencing factors of residual stresses in selective laser melting using a novel analysis method," *Proceedings of the Institution of Mechanical Engineers - Part B: Journal of Engineering Manufacture*, vol. 226, no. 6, pp. 980–991, 2012.

[21] R. Acevedo, P. Sedlak, R. Kolman, and M. Fredel, "Residual stress analysis of additive manufacturing of metallic parts using ultrasonic waves: state of the art review," *Journal of Materials Research and Technology*, vol. 9, no. 4, pp. 9457–9477, 2020.

[22] D. Wang, S. Wu, Y. Yang et al., "The effect of a scanning strategy on the residual stress of 316L steel parts fabricated by selective laser melting (SLM)," *Materials*, vol. 11, no. 10, 1821 pages, 2018.

[23] X. Gong, D. Zeng, W. Groeneveld-Meijer, and G. Manogharan, "Additive manufacturing: a machine learning model of process-structure-property linkages for machining behavior of Ti-6Al-4V," *Materials Science in Additive Manufacturing*, vol. 1, no. 1, 6 pages, 2022.

[24] A. Khobzi, F. Farhang Mehr, S. Cockcroft, D. Maijer, S. L. Sing, and W. Y. Yeong, "The role of block-type support structure design on the thermal field and deformation in components fabricated by Laser Powder Bed Fusion," *Additive Manufacturing*, vol. 51, Article ID 102644, 2022.

[25] A. S. Wu, D. Brown W, M. Kumar, G. F. Gallegos, and W. E. King, "An experimental investigation into additive manufacturing-induced residual stresses in 316L stainless steel," *Metallurgical and Materials Transactions A: Physical Metallurgy and Materials Science*, vol. 45, pp. 1–11, 2014.

[26] I. Yadroitsev and I. Yadroitsava, "Evaluation of residual stress in stainless steel 316L and Ti6Al4V samples produced by selective laser melting," *Virtual and Physical Prototyping*, vol. 10, no. 2, pp. 67–76, 2015.

[27] S. D. Bagg, L. M. Sochalski-Kolbus, and J. R. Bunn, "The Effect of Laser Scan Strategy on Distortion and Residual Stresses of

Arches Made with Selective Laser Melting," in *Proceedings of the American Society of Precision Engineering (ASPE) 2016 Summer Topical Meeting*, Huntsville, AL, USA, July 2016.

[28] T. Mishurova, S. Cabeza, K. Artzt et al., "An assessment of subsurface residual stress analysis in SLM ti-6Al-4V," *Materials*, vol. 10, no. 4, 348 pages, 2017.

[29] S. I. Kim and A. J. Hart, "A spiral laser scanning routine for powder bed fusion inspired by natural predator-prey behaviour," *Virtual and Physical Prototyping*, vol. 17, no. 2, pp. 239–255, 2022.

[30] A. G. Dharmawan and G. S. Soh, "A cylindrical path planning approach for additive manufacturing of revolved components," *Materials Science in Additive Manufacturing*, vol. 1, no. 1, p. 3, 2022.